Available online www.jsaer.com

***Journal of Scientific and Engineering Research*, 2018, 5(5):207-219**

Research Article

ISSN: 2394-2630
CODEN(USA): JSERBR

Energy Characterization of PV/T based Water Pumping and Heating System

Majed BEN AMMAR[1], Mohsen BEN AMMAR[2]

[1]University of Gabes, Higher Institute of Industrial Systems (ISSIG), Rue, Slaheddine El Ayoubi, 6032 Gabès-Tunisia
[2]CEM-Lab, University of Sfax, National Engineering School of Sfax (ENIS), Route de Soukra km 4 Sfax – B.P. 1173, 3038 Sfax-Tunisia

Abstract In this paper, an integrated combined system of photovoltaic thermal (PV/T) solar pumping heating water in outdoor condition was modeled for some considered distribution of climatic parameters. An analytical expression for the energy balance, which includes the photo conversion and heat transfer coefficients for PV/T collector has been derived for different conditions as a function of design and climatic parameters. The testing of this system was carried out during August–November, 2017. The dynamic behavior of states and outputs system was monitored. The investigation of these results on PV/T performance has been carried out.

Keywords Photovoltaic thermal (PV/T), dynamic behavior, PV/T performance

1. Introduction

The efficiency of the photovoltaic panel is commonly know to decrease when the cell temperature increases. Motivated by the fact that a solar collector can transform the heat captured by its surface into a coolant, a new technology combining these two approaches (Photovoltaic/Thermal PV/T) has been developed. In fact, this hybrid system allows to simultaneously produce electrical, thermal energy and decrease the cell temperature by the water/air circulation. Over the previous few years, a large amount of research on hybrid PV/T panels has been conducted. PV/T panels are used for both air heating [1, 2] and water heating pumping [3, 4]. This technology has been studied theoretically [5-7] and experimentally [8-10].

An experimental investigation was conducted to study the thermal and electrical efficiency of PV/T and PV/T-PCM panels. This study confirms that the use of phase change materials (PCMs) can effectively reduce the cell temperature and consequently increase the performance of the system [11]. In addition, a concentrated PV/T solar system using linear Fresnel lens was proposed. As a result of solar concentration, the PV module characteristic indicates that the *10.9%* PV cells electrical efficiency decreases to *7.63%* under normal condition [12]. Another experimental study and analysis was performed on the CPC-PV/T system on constant temperature and flow operations. The advantages and drawbacks of the two operation modes show the coupling effect of PV/T with CPC [13]. PV/T systems were analyzed at a PV string level. Different operating conditions were tested and the electrical and thermal critical operating conditions were investigated. [14]

Several theoretical studies dealing with the PV/T system performance have been achieved. In [15], a comprehensive optimization of a PV/T active solar still was carried out and the optimized value of the mass flow rate as well as number of PV/T collectors and the energy efficiency of PV/T active solar still was obtained. A steady-state model was proposed, showing the effect of various parameters on the still performance of the new concentrated solar PV/T distillation system. The obtained performance curves showed the effect of wind speed, solar intensity, ambient temperature, condenser temperature, and PV cell [16]. Besides, a dynamic model of the PV/T collector with dual channels for different fluids was developed and the performance parameters

were derived to carry out comparative analyses [17]. A Support vector machine (SVM) model was analyzed for the prediction of the electrical and thermal performance in a PV/T system. A proper sensitivity analysis was also performed to identify the influence of the considered input elements on the prediction of the PV/T system performance. [18]

In the present research, a theoretical study was conducted on the dynamic behavior of water pumping heating system. The energy balance equation of each component of the PV/T panel was simulated using Matlab software. The model generated results for hourly and transient performance analysis. Consequently, the PV/T system energy characterization has been established for different climatic parameters.

Nomenclature

A	Surface area, m^2
C	Specific heat capacity, *J/(kg K)*
E	Electrical power, *Watt*
g	Gravitational constant, *9.81 m/s²*
h	Heat transfer coefficient, *W/m² K*
h_r	Radiation heat transfer coefficient , *W/m²*
I	Current, *A*
I_r	Solar radiation intensity, *W/m²*
K	Insulation thermal conductivity, *W/m K*
k_1	Plate thermal conductivity, *W/m K*
L	Length of the tube, *m*
$\dot{m}$	Mass flow rate, *kg/s*
M	Mass, *kg*
N_u	Nusselt number,
Q	Thermal energy, *Wh*
R_e	Reynold number,
T	Temperature, *K*
t	Time, *s*
v	Wind sped, *m/s*
V	Voltage, V
y	Travelling distance, *m*

Greek

α	Absorptance
β	Vertical orientation angle, *45°*
β_g	PVG temperature coefficient, *0.0045°C⁻¹*
ε	Emissivity
η	Efficiency
σ	Constant of Stefan,*5.6696× 10⁻⁸W/m²K⁴*
τ	Transmissivity
β'	Volumetric coefficient
υ	Viscosité cinématique du fluide, *m²/s*

Superscript

+	Critical
$[\ ]^T$	Transpose

Subscripts

a	Ambient air
c	Solar cell
f	Fluid
g	Glass cover
p	Absorber plate
i	Inlet

2. Structure of PV/T panel

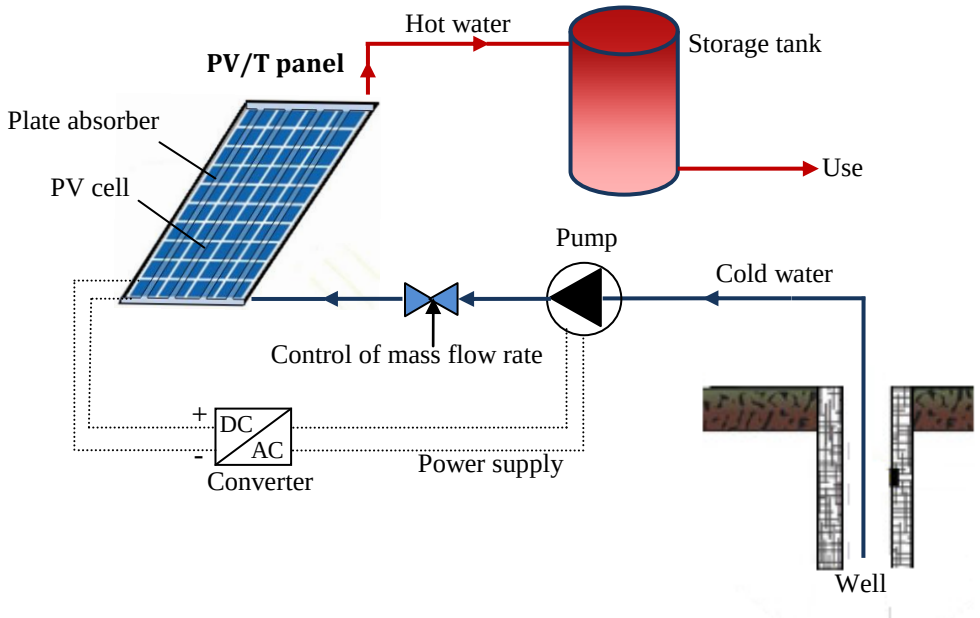

Figure 1: Schematic diagram of water heating pumping system

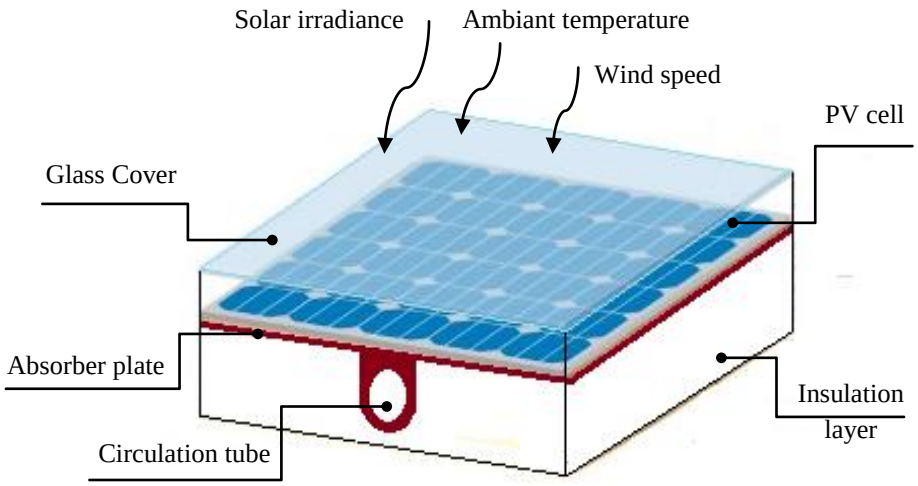

Figure 2: Sectional view of PV/T panel

The schematics diagram of the water pumping and heating system is shown in Fig. 1. It includes a water storage tank joined to the PV/T panel. A water pump supplied with the PV/T generated electric power ensures the water circulation.

The configuration of the PV/T panel is shown in Fig. 2. This panel is basically constructed by pasting photovoltaic solar cells directly over the absorber plate of the solar collector in conventional forced circulation type using a solar water heater.

3. PV/T panel numerical approach

The mathematical model of PV/T panel is based on four nodes:

(i) ***Node 1***: A transparent cover allowing sunlight to pass towards the absorber and to create a greenhouse effect, characterized by glass temperature T_g.

(ii) ***Node 2***: A photovoltaic cell for the production of electricity, characterized by cell temperature T_c.

(iii) ***Node 3***: An absrbing plate that transform the collected energy into a coolant, characterized by absorber plate temperature T_p.

(iv) ***Node 4***: A fluid circulation canal, characterized by water temperature T_f.

Figure 3 shows the electrical-thermal analogy between the different components of PV/T panel.

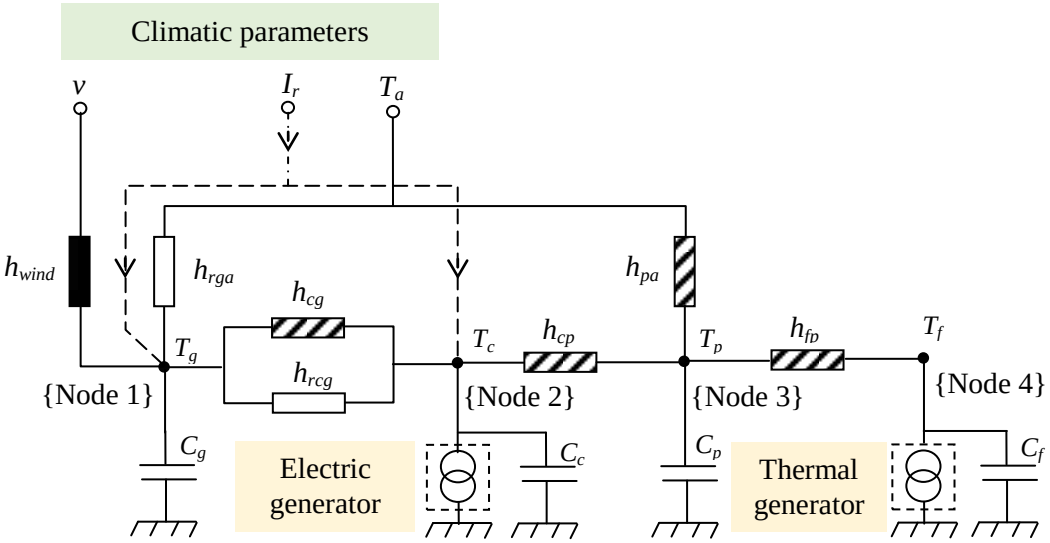

Figure 3: Electrical/thermal PV/T collector model

Where T_i and C_i are respectively the specific temperatures and heats of each node, I_r is the solar irradiance, T_a is the ambient temperature, v is the wind speed, h_{ij} and h_{rij} are respectively the transfer coefficients by convection and by radiation between the nodes i and j in $(W/m^2.K)$. Based on the electrical/thermal model, the state representation model of PV/T panel is given in Figure 4.

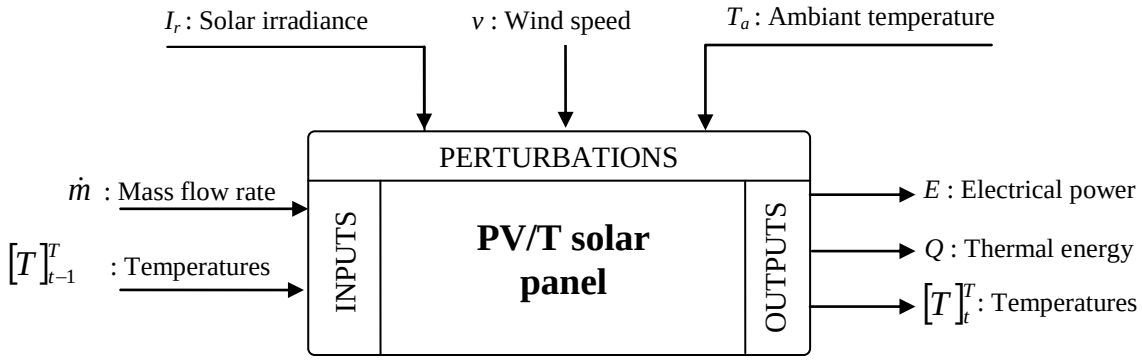

Figure 4: PV/T panel synoptic diagram.

At constant wind speed v= *1m/s*, the input vector is $T=[T_g \;\; T_c \;\; T_p \;\; T_f]^T$ containing the temperatures at the four nodes of the PV/T system, the perturbation input $W=[I_r \;\; T_a]^T$ containing the solar radiation I_r and the ambient temperature T_a. $Y=[E \;\; Q]^T$ is the output vector containing the electrical powers and the thermal profit gain. This PV/T system is controlled by a mass flow rate $\dot{m}$.

4. PV/T panel energy balance

A functional approach combing the different subsets was used in order to evaluate the transient regimes of the various internal quantities of the system. The equations of the central nodes and the conductance are respectively determined by:

$$\sum_{j}^{i} K_{ij} \times (T_j - T_i) = 0 \tag{1}$$

$$K_{ij} = h_{ij} \cdot S_{ij} \tag{2}$$

Where S_{ij} is the exchange surfaces between i and j layers. The following assumptions were considered in the model development:

- The mass flow rate of the working fluid is invariant in all tube sections.
- All the PV/T system component material properties are unchanged.
- The heat transfer coefficients were computed in real time

The energy balance for each component of the PV/T collector is given in Table 1.

Table 1: The PV/T system energy balance

Node 1: Glass cover sub model	
$M_g C_g \dfrac{dT_g}{dt} = \alpha_g I_r A_g + A_g (h_{wind} + h_{rga})(T_a - T_g) + A_g h_{rgc}(T_c - T_g) + A_g h_{gc}(T_c - T_g)$	(3)
Node 2: Solar cell sub model	
$M_c C_c \dfrac{dT_c}{dt} = (\alpha_c \tau_g A_c (1 - \eta_c)) I_r - A_g . h_{rcg}(T_c - T_g) - A_g . h_{cg}(T_c - T_g) - A_c h_{cp}(T_c - T_p)$	(4)
Node 3: Absorber plate sub model	
$M_p C_p \dfrac{dT_p}{dt} = A_c . h_{cp}(T_c - T_p) - A_c . h_{pa}(T_p - T_a) - A_f h_{fa}(T_f - T_a) - \dot{m} . C_f \Delta T_f$	(5)

Node 4: Water in channels sub model

$$M_f C_f \frac{dT_f}{dt} = A_f h_{pf}(T_p - T_f) - C_f \dot{m} \frac{\Delta T_f}{\Delta y} \quad (6)$$

Where M_i is the mass of the front glazing, solar cell, absorber plate and fluid of PV/T panel, α_i represents the effective glass and solar cell absorptivity, h_{cg} the convective heat transfer coefficients between the solar cell and the glass cover [19].

The convective heat transfer coefficient wind speed is given by:

$$h_{wind} = 2.8 + 3 \times v \quad (7)$$

The radiation heat transfer coefficient between the front cover and the ambient environment is:

$$h_{rga} = \varepsilon_g \times \sigma \times (T_g^2 + T_a^2) \times (T_g + T_a) \quad (8)$$

In addition the radiation heat transfer between the glass cover and the PV cells is expressed as follows:

$$h_{rgc} = \sigma \times (T_g^2 + T_a^2) \times (T_g + T_a) / (\frac{1}{\varepsilon_g} + \frac{1}{\varepsilon_c} - 1) \quad (9)$$

Where ε_g and ε_p are the emissivity of the glazing and the collector plate respectively, σ is the Stefan-Boltzmann constant, and *y* is the channel length. The convective heat transfer between cell and absorber plate is:

$$h_{cp} = N_u \frac{k_1}{L} \quad (10)$$

Hollands et al., 1976 determined the Nausselt number by the following equation:

$$N_u = 1 + 1.44\left[1 - \frac{1708 \times (\sin 1.8\beta)^{1.6}}{R_e \cos\beta}\right] \times \left[1 - \frac{1708}{R_e \cos\beta}\right] + \left[\left(\frac{R_e \cos\beta}{5830}\right)^{1/3} - 1\right] \quad (11)$$

The Reynolds number is given by:

$$R_e = \frac{g\beta' \Delta T L^3}{\upsilon\alpha} \quad (12)$$

Where the difference in temperature of the cell/collector surface and temperature of the plate (bottom) is:

$$\Delta T = (T_p - T_c) \quad (13)$$

The volumetric coefficient is:

$$\beta' = 1/T_a \quad (14)$$

Where h_{pa} is the conduction heat transfer coefficient between the absorber and the ambient environment, h_{fa} the water flow in channel convective heat transfer coefficient. Based on the analogical diagram and the energy balance of the PV/T panel, the state equation (SE) is:

$$SE: \begin{cases} \dot{T} = AT + BU + DW \\ Y = CT \end{cases} \quad (15)$$

Where *A* and *C* are respectively the state and output matrices which contain the heat exchange coefficients between the system elements, *B* is the control matrix which includes the commands applied on the mass flow rate ($\dot{m}$), *D* is the perturbation matrix acting on the perturbation inputs vector.

5. PV/T panel energy and efficiency

The equivalent circuit of the general model consists of a photo current, a diode, a parallel resistor expressing the leakage current, and a series resistor describing an internal resistance to the current flow. The PV circuit is connected to the load (R_L) via a boost converter which tracks the maximum power point.

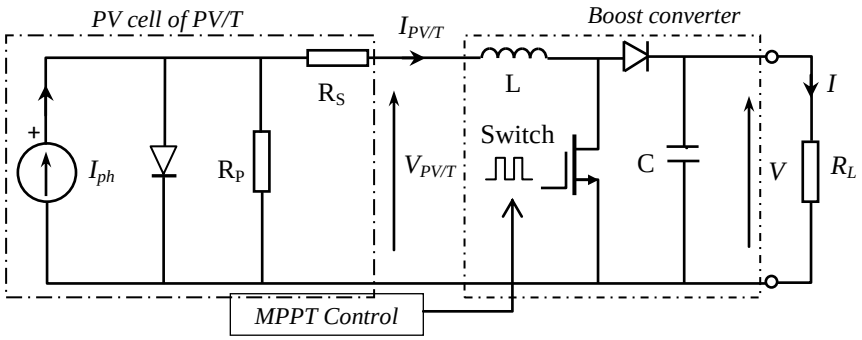

Figure 5: The PV/T panel equivalent circuit model

The electric power output depends on the instantaneous operating temperature T_c of the PV module, and can be expressed as the electrical current function of the PV module [20]. The current model of a solar cell is given by:

$$I_{PV/T} = I_{sc}\{1-[C_1 \exp(V_{PV}/(C_2 \times V_{oc}))-1]\} + \Delta I \quad (16)$$

Where V_{oc} is open circuit voltage, I_{sc} is the short circuit current and ΔI is the current variation.

$$C_1 = (1 - V_{mpp}/I_{sc}) \times \exp(-V_{mpp}/(C_2 \times V_{oc})) \quad (17)$$

And $$C_2 = ((V_{mpp}/V_{oc})-1)/\ln(1-(I_{mpp}/I_{sc})) \quad (18)$$

The current variation is given by:

$$\Delta I = (\alpha_{sc} \times (I_r / I_{r,STC}) \times \Delta T) + I_{sc} \times ((I_r / I_{r,STC}) - 1) \quad (19)$$

Where α_{sc} and $I_{r,STC}$ are respectively the absorptance of the solar cell and the solar radiation in standard condition. The difference in temperature of the cell/collector surface and temperature in standard test condition (STC : AM = 1.5, I_r = 1000 W/m^2 and T_c = 25°C) is:

$$\Delta T = T_c - T_{STC} \quad (20)$$

The PV output voltage of PV/T panel is expressed by a dynamic equation as:

$$V_{PV/T} = V_{mpp} \times (1 + 0.0539 \times \ln(I_r / I_{r,STC})) + \beta_{oct} \times \Delta T - R_S \times \Delta I \quad (21)$$

Where R_S and β_{oct} are respectively the internal serial resistance relative to one cell and the temperature cell coefficient in an open circuit voltage and V_{mpp} is the maximum power point.

The electrical power produced by the PV/T module, formed by N_S serial cells and N_p parallel cells, is calculated by the following expression:

$$E = N_s \cdot N_p \times V_{PV/T} \times I_{PV/T} \quad (22)$$

The PV cells efficiency is determined by:

$$\eta_{pv} = \eta_r [1 - \beta_g (T_c - T_r)] \quad (23)$$

Where η_r and β_g are respectively the reference efficiency and the temperature coefficient of the PV/T collector.

The PV/T panel thermal energy output depending on the instantaneous operating temperature T_f is expressed by : [19]

$$Q = \dot{m} C_f (T_f - T_{fi}) \quad (24)$$

The thermal efficiency is determined according to the thermal energy :

$$\eta_{th} = \frac{Q}{A_c \int I_r \times dt} = \frac{\dot{m} \times C_f \times \int (T_f - T_{fi}) \times dt}{A_c \int I_r \times dt} \quad (25)$$

The total efficiency of PV/T panel is expressed by :

$$\eta_{pvt} = \eta_{th} + \eta_{pv} \quad (26)$$

6. Results and Discussion

The PV/T collector climatic, operating and design parameters during the validation process are described in Table 2.

Table 2: PV/T collector design parameters

Front glazing	***Value***	Nominal current I_{mpp}	*5.2 A*
Area of glass	*1.66 m^2*	Open circuit voltage V_{oc}	*45.2 V*
Mass of glass	*8.3 kg*	Current in standard conditions I_{sc}	*5.61A*
Glass specific heat capacity	*810 J/kg K*	***Thermal absorber (cuivre)***	***Value***
Glass emissivity	*0.88*	Absorbing plate area	*1.55 m^2*
Glass tranmissivity	*0.95*	Absorbing plate mass	*9012 kg*
		Absorber material	*386 W/m°C*
Solar cell (monocristallin)	***Value***	Absorbing plate specific	
Cell area	*1.37 m^2*	heat capacity	*900J/kg K*
Cell mass	*6.1 kg*	***Water in channel***	***Value***
Cells size	*6'', 125mm/125mm*	Channel fluid circulation area	*0.156 m^2*
Cell specific heat capacity	*901 J/kg K*	Water mass	*45 kg*
Cell emissivity	*0.88*	Fluid specific heat capacity	*1005 J/kg K*
PVG reference temperature	*298K*	Tubes number	*10*
Vertical orientation angle	*45°*	Tube length	*1 m*
Current in standard conditions	*5.61*	Distance between tubes	*0.2 m*
Temperature coefficient	*300K*	***Heat transfer coefficient***	***Value***
Number of modules in parallel	*33*	h_{pf}	*100 W/m^2K*
Cell number	*60*	h_{fa}	*1000W/m^2K*
Nominal power P_{mpp}	*170 Wc*	h_{pa}	*5.7 W/m^2K*
Nominal voltage V_{mpp}	*36.4 V*	h_{cg}	*100 W/m^2K*

6.1. PV/T system dynamic behavior

The modeled system was tested for the considered distribution of solar radiation and ambient temperature. The simulation was performed using MATLAB. The behavior for different constituents and the transient performance of the PV/T system was simulated at a time step of one minute during two typical days: a cold season day and a hot season day.

For each day, the water and cell temperature instantaneous variations were simulated according to the climatic parameters distribution. At a constant mass flow rate ($\dot{m}$ = *144 l/h*), the output data were evaluated and used to estimate the electrical and thermal efficiency of PV/T system. Figures 6 and 7 show the dynamic comportment of the PV/T for a constant wind speed (v = *1 m/s*).

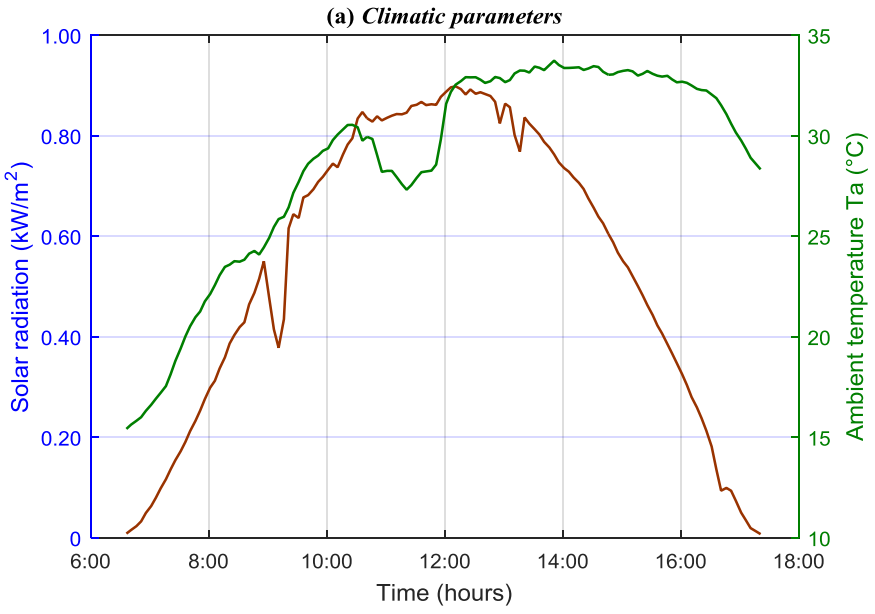

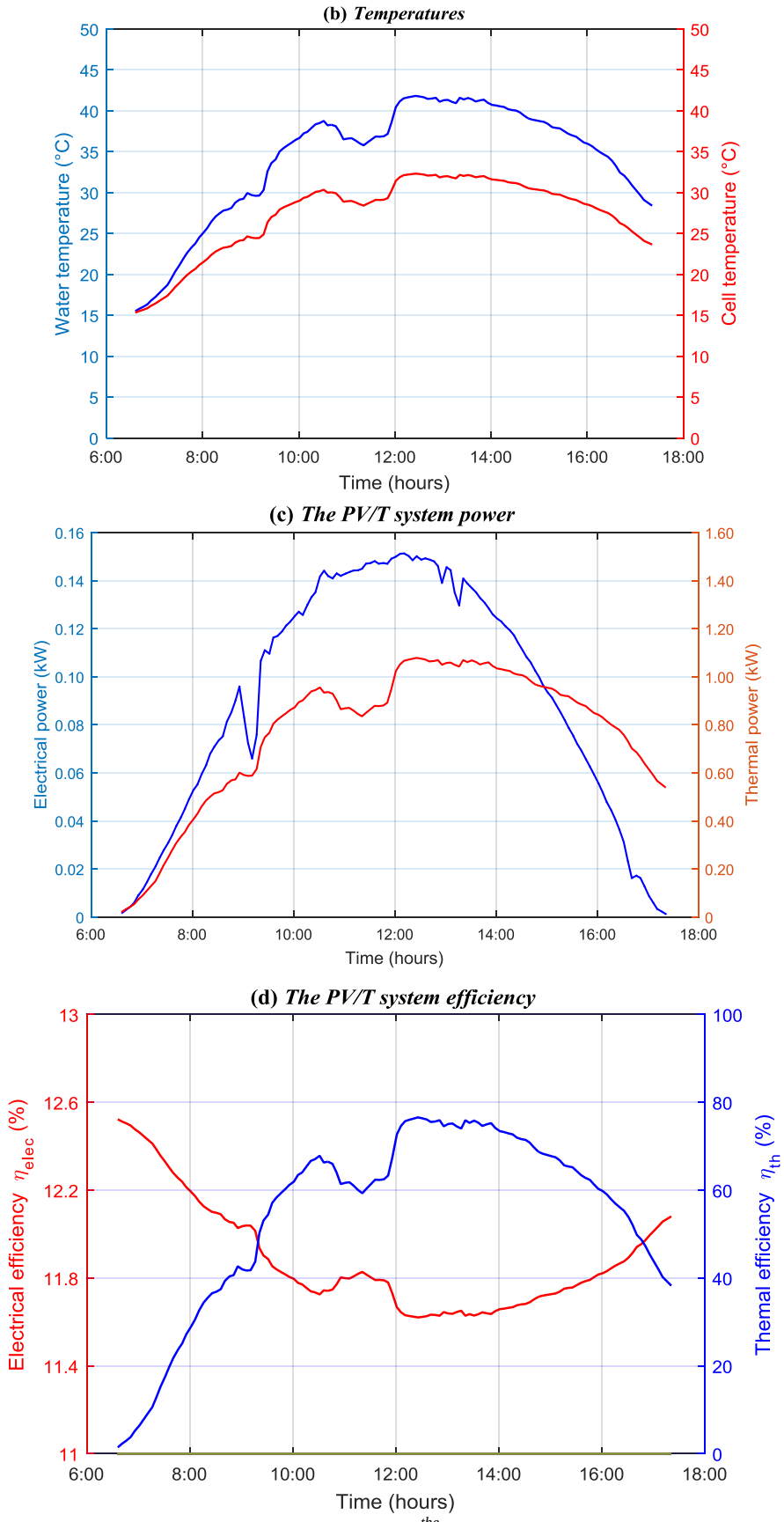

Figure 6: Characterization of the PV/T system (August 22^{the} 2017 as a representative day of the hot season).

A typical day of the summer (August 22th, 2017) was considered to simulate the PV/T model during the hot season. For a given design and the solar radiation and ambient temperature distribution, the hourly variation of the theoretical outlet temperature results are shown in Fig. 6(b). The electrical power and thermal energy were evaluated using equations 22 and 24. These electrical power and thermal energy are shown in Fig 6.(c), It is clear that there is a good agreement between inputs temperatures and outputs powers.

Similarly, Equations 23 and 25 have been computed to evaluated the instantaneous efficiency during the month of August. The dynamic thermal and electrical efficiency behaviours are shown in Fig. 6 (d). The same figure shows that the cell temperature increase decreases the electrical efficiency, and that the water temperature decrease causes the thermal energy to drop.

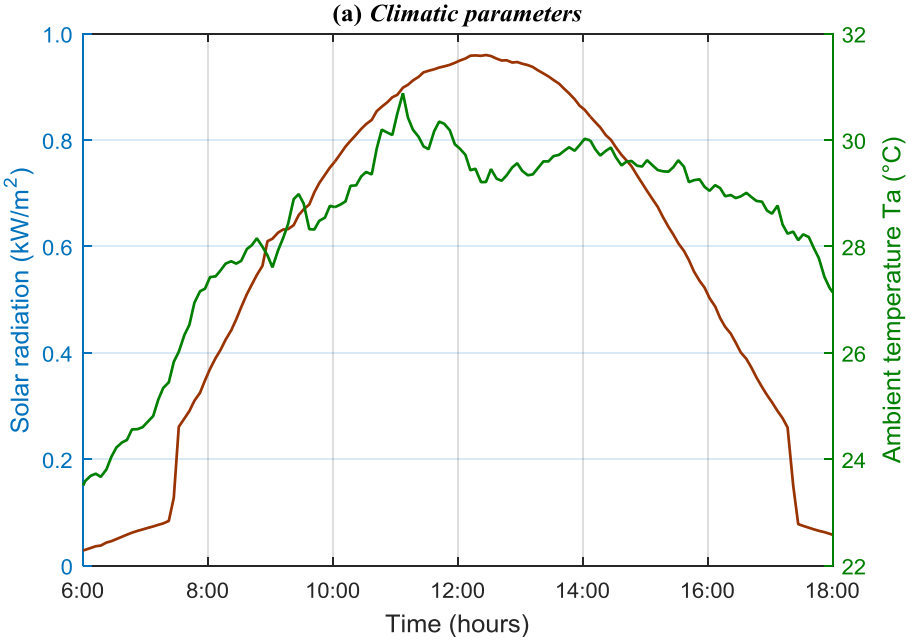

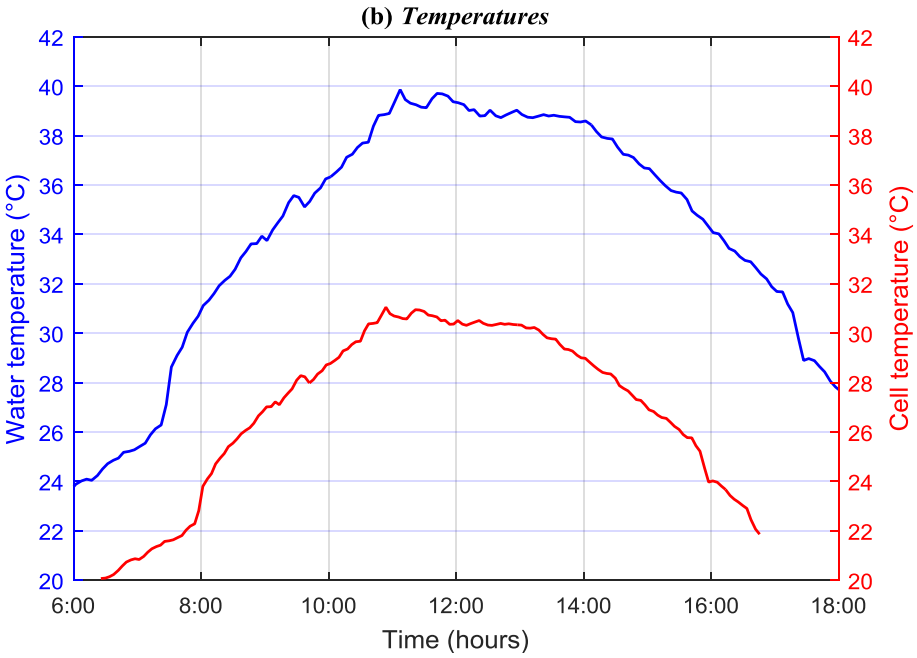

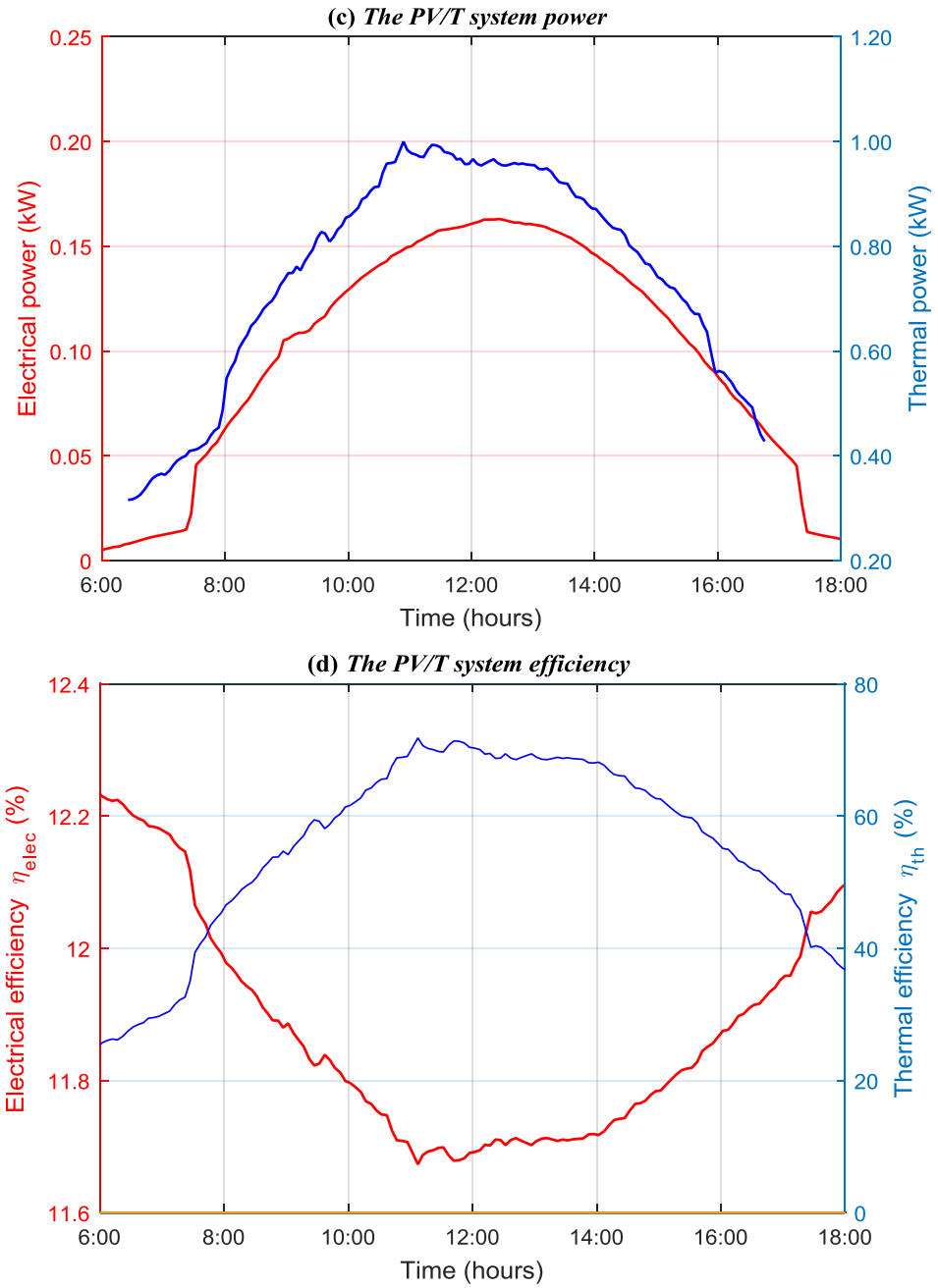

Figure 7: Characterization of the PV/T system (November 22^{the} 2017 as a representative day of the cold season).

Similar simulations to those described in the previous paragraph were achieved during a typical day in the month of November. Fig. 7 (b) displays the temperatures behavior. These results reveal that, when the solar radiation and ambient temperature increase, the water and cell temperatures rise to reach 31°C and 39°C (at 12:00). Figures 7 (c) and 7 (d) respectively show the PV/T system energy and efficiency at constant mass flow rate. The obtained results reveal that when the electrical efficiency decreases from 12.2% to 11.66%, the thermal efficiency increases from 22% to 69% (at 12:00)

6.2. PV/T system electrical characteristic

The PV/T system electrical characteristic varies according the instantaneous cell temperature. Figures 8 and 9 show these characteristics for different values of solar radiations and ambient temperature.

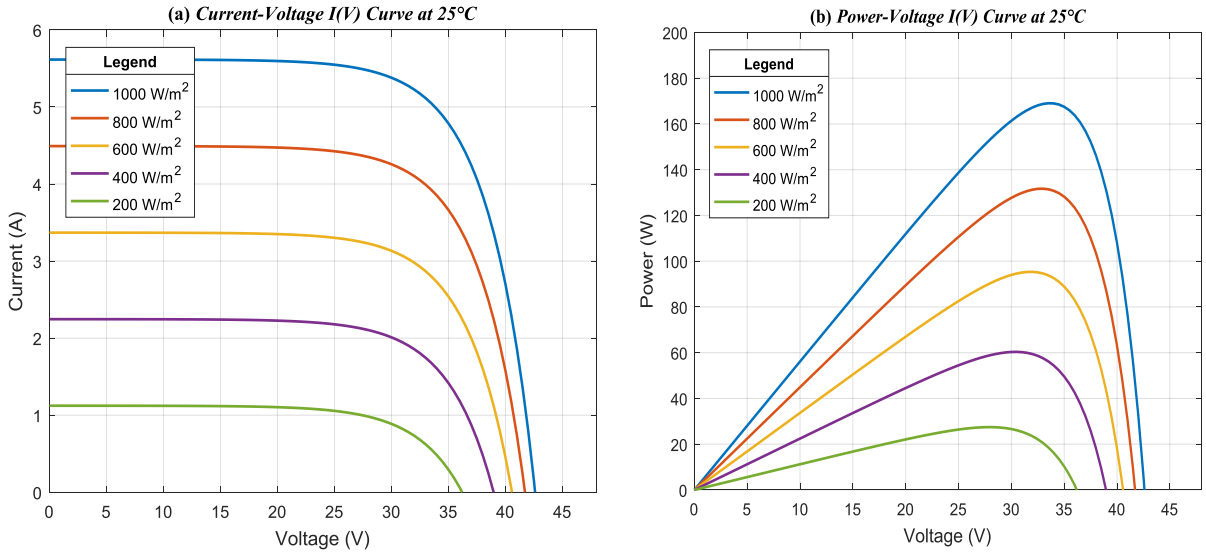

Figure 8: The PV/T system electrical characteristics for different solar radiation values

Fig. 8 shows the electrical characteristic for several solar radiation values which vary between *200 W/m²* and *1000W/m²* and for a constant temperature equal to *25 °C*. The current and the power are remarked to increase with the decrease of the radiation. However, both of the short circuit and open circuit voltage are variable.[21]

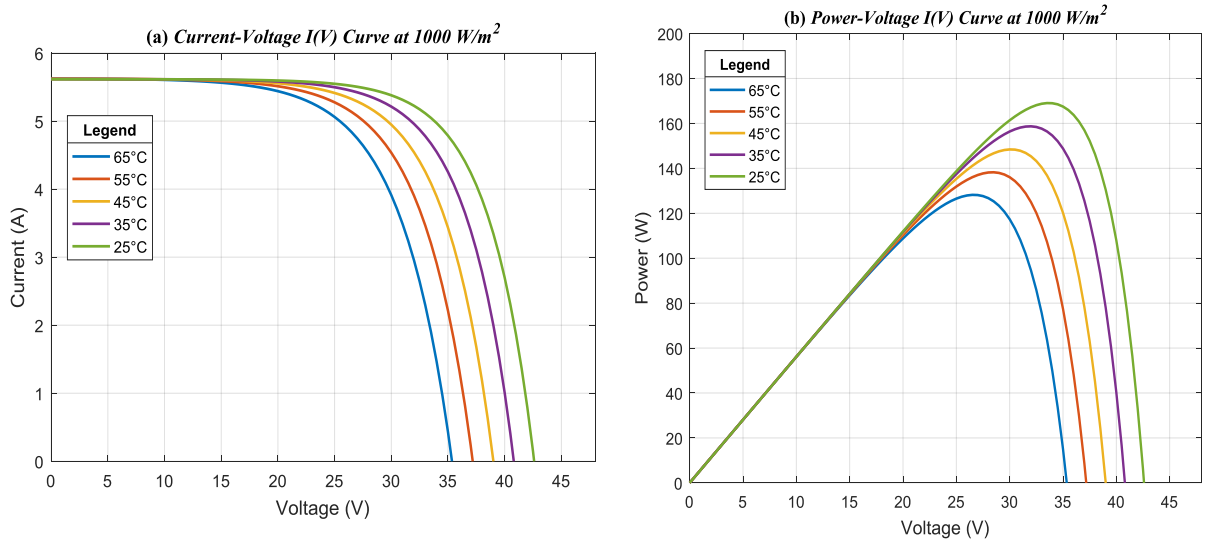

Figure 9: The PV/T system electrical characteristics for different ambiant temperature values

Fig. 9 shows the simulation results of I-V and P-V characteristics respectively under the same conditions for different ambiant temperature values (*25°C, 35°C, 45°C, 55°C, 65°C*) at constant solar radiation *1000W/m²*. The generated current by the solar radiation remains constant although it increases slightly while the voltage decreases. Thus, the power increases when the voltage increases. [20]

6.3. Mass flow rate effect on the PV/T system performance

The PV/T system tempertaure decreases while the mass flow rate increases (Eq. 3,4,5 and 6). Consequently, the electrical efficiency increases while the cell temperature decreases (Eq. 23) and the thermal efficiency decreases while the water temperature increases (Eq. 25). These observations will be maintained by compiling the PV/T model simulated for different mass flow rates ($\dot{m}$ = *54 l/h*, $\dot{m}$ = *90 l/h*, $\dot{m}$ = *126 l/h*) during the month of June.

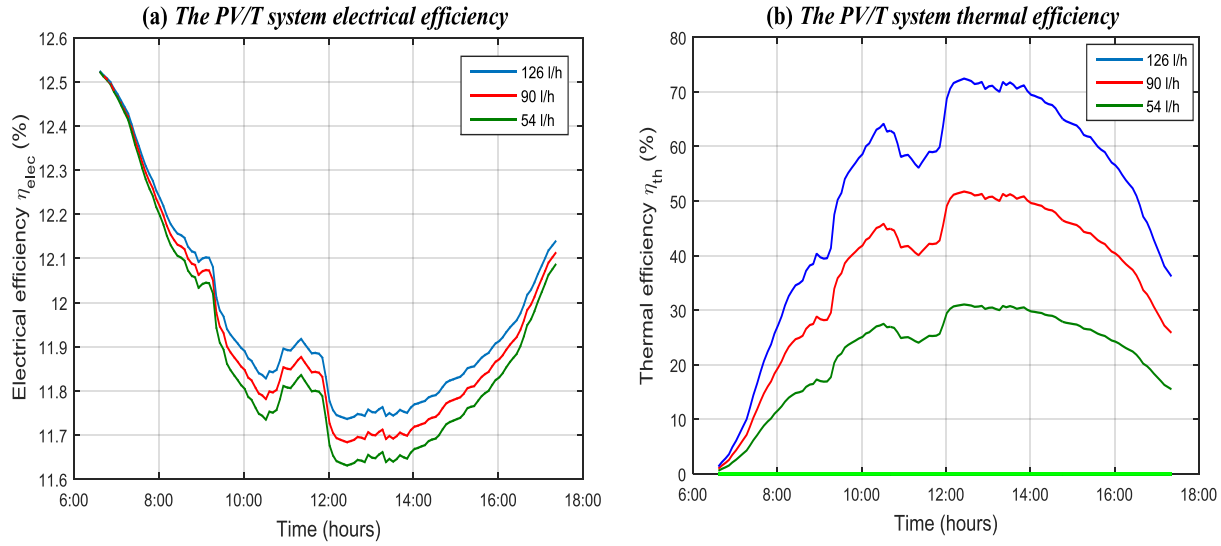

Figure 10: The PV/T system Efficiency at different mass flow rates (June, 22th 2017)

The mass flow rate has to be considered as an important factor which influences the electrical and thermal efficiencies of the PV/T system. The hourly variation of these efficiencies for various mass flow rate values of are shown in Fig 10. These results reveal that, when $\dot{m}$ increases from *54 l/h* to *126 l/h*, the electrical efficiency increases from *11.66%* to *11.79%* at *12:00* and the thermal efficiency rises from *37%* to *64%* at *12:00*.

7. Conclusion

This work has allowed us to study the PVT panel by determining the thermal and electrical energy, such as cell temperature and water temperature, electrical and thermal efficiency, for different ambient temperature and solar radiation values. The obtained results suggest that it is a good alternative to photovoltaic and conventional thermal panel generators separately installed. The extracted heat could then be used to heat the water. Also, we would increase the electrical efficiency and exploit the collected thermal energy.

Acknowledgements

This work was funded by the ministry of higher education of Tunisia. We also would like to thank Mr Abdelmajid damak, an english teacher at Sfax National School of engineers, Tunisia, for his help with the proofreading this paper.

References

[1]. Chihong Cao, Huixing Li, Guohu iFeng, Ran Zhang, Kailiang Huang. Research on PV/T – Air Source Heat Pump Integrated Heating System in Severe Cold Region. Procedia Engineering 2016; 146: 410 – 414.

[2]. Gang Wang, Zhenhua Quan, Yaohua Zhao, Chenming Sun, Yuechao Deng, Jiannan Tong. Experimental study on a novel PV/T air dual-heat-source composite heat pump hot water system. Energy and Buildings 2015; 108: 175–184.

[3]. JianboQin, Xianghua Jiang, Yunting Ge. Experimental investigation of gas bubble diameter distribution in a domestic heat pump water heating system. Energy Procedia 2017; 123: 361–368.

[4]. Xiaolin Sun, Jingyi Wu, Yanjun Dai, Ruzhu Wang. Experimental study on roll-bond collector/evaporator with optimize dchannel used in direct expansion solar assisted heat pump water heating system. Applied Thermal Engineering 2014; 66 : 571-579.

[5]. Zhongzhu Qiu, Xudong Zhao, Peng Li, Xingxing Zhang, Samira Ali, Junyi Tan. Theoretical investigation of the energy performance of a novel MPCM (Microencapsulated Phase Change Material) slurry based PV/T module. Energy 2015; 87 : 686-698.

[6]. S.A. Kalogirou, Y. Tripanagnostopoulos. Hybrid PV/T solar systems for domestic hot water and electricity production. Energy Conversion and Management 2006; 47: 3368–3382.
[7]. Pei Gang, Fu Huide, Ji Jie, Chow Tin-tai, Zhang Tao. Annual analysis of heat pipe PV/T systems for domestic hot water and electricity production. Energy Conversion and Management 2012; 56: 8–21.
[8]. Jie Ji, Yanqiu Wang, Weiqi Yuan, Wei Sun, Wei He, Chao Guo. Experimental comparison of two PV direct-coupled solar water heating systems with the traditional system. Applied Energy 2014; 136: 110–118.
[9]. Mohammad Sardarabadi, Mohammad Passandideh, Saeed Zeinali Heris. Experimental investigation of the effects of silica/water nanofluid on PV/T (photovoltaic thermal units). Energy 2014; 66: 264-272.
[10]. Ben cheikh el hocine H , Touafek K , Kerrour F , Haloui H , Khelifa A. Model Validation of an Empirical Photovoltaic Thermal (PV/T) Collector. Energy Procedia 2015; 74: 1090 – 1099.
[11]. Xiaojiao Yang, Liangliang Sun, Yanping Yuan, Xudong Zhao, Xiaoling Cao. Experimental investigation on performance comparison of PV/T-PCM system and PV/T system. Doi: 10.1016/j.renene.2017.11.094. Renewable Energy 2017.
[12]. Fariborz Karimi, Hongtao Xu, Zhiyun Wang, Jian Chen, MoYang. Experimental study of a concentrated PV/T system using linear Fresnel lens. Energy 2017; 123: 402-412
[13]. Zhang Henga, Li Mingjiea, Chen Haipinga, Ye Chentaoa. Experimental study of constant temperature operation and constant flow operation in concentrating PV / T system. Energy Procedia 2017; 105: 869–874.
[14]. M. Rosa-Clot, P. Rosa-Clot, G.M. Tina, C. Ventura. Experimental photovoltaic-thermal Power Plants based on TESPI panel. Solar Energy 2016; 133: 305–314.
[15]. F. Saeedi, F. Sarhaddi, A. Behzadmehr. Optimization of a PV/T (photovoltaic/thermal) active solar still. Energy 2015; 87: 142-152.
[16]. Moh'd A. Al-Nimr, Moh'd-Eslam Dahdolan. Modeling of a novel concentrated PV/T distillation system enhanced with a porous evaporator and an internal condenser. Solar Energy 2015; 120: 593–602.
[17]. Di Su, Yuting Jia, Xiang Huang, Guruprasad Alva, Yaojie Tang, Guiyin Fang. Dynamic performance analysis of photovoltaic–thermal solar collector with dual channels for different fluids. Energy Conversion and Management 2016; 120: 13–24.
[18]. Juwel Chandra Mojumder, Hwai Chyuan Onga, Wen Tong Chonga, Shahaboddin Shamshirband, Abdulla Al Mamoona. Application of support vector machine for prediction of electrical and thermal performance in PV/T system. Energy and Buildings 2016; 111: 267–277.
[19]. John A. Duffie (deceased), William A. Beckmann. Solar engineering of thermal processes. Fourth Edition. ISBN 978-1-118-67160-3, Solar Energy Laboratory University of Wisconsin-Madison New York Wiley; 2013.
[20]. Mohsen BenAmmar, Maher Chaabene, Ahmed Elhajjaji. Daily energy planning of household photovoltaic panel. Applied Energy, 2010, vol. 87, issue 7, 2340-2351.